Friction calibration in die metallic interface and stress analysis of steel [AISI 1010] employing ring compression test under specified lubrication

Asst. Prof. Libin Kochumman, Prof.M.R. Sarathchandradas

Abstract -The main objective of this paper is to investigate the effect of barreling on the behaviour of friction calibration curves. In the metal forming process, a realistic frictional condition must be specified at the die/work piece interface in order to obtain accurate metal flow. Several methods are developed to evaluate friction in large deformation processes. This paper presents the concept of friction calibration map to determine different frictional conditions between interfaces of die and billet in the upsetting process. These maps are generated based on the finite element simulation studies. A series of ring compression tests were then conducted to obtain the friction calibration curve. According to the Male and Cockcroft the standard geometry (6: 3 :2)is modelled with outer diameter 30mm, inner diameter 15mm and height 10mm. The simulation were first conducted for the modelling material, steel [AISI 1010], and were simulated using nonlinear analysis finite element code (ANSYS). For different height reduction and friction coefficients is provided for simulation, the profile changes for inner surface node are investigated and friction calibration curve is obtained. Ring compression test is carried out experimentally and the results are compared with the numerical results and validated. The deformation and stress variation study is carried out for the inner radius of the ring and barrelling effect is defined by the deformation profile and stress variation analysis.

Index Terms—Barreling, Friction Calibration, Finite element method, Ring compression test

1 INTRODUCTION

Friction plays vital role in all metal working process because of its direct interaction between die and work piece. Friction is predominantly the effect of the high pressures used and surface finish in both dies and work piece interface. The unavoidable friction obstructs free movement at interfaces and further it significantly affects the flow and deformation of the work piece. Thus prediction of coefficient of friction between the die and the billet interface become important, in order to avoid the need for secondary processing to remove small amounts of billet materials by machining and to reduce defects due to improper material flow. The coefficient of friction is usually determined either by experimental methods or by simulation using specimens of various shapes.

There are several tests, reported in literature, to evaluate friction. Most popular among them is the Ring Compression Test. It was proposed by Male and Cockcroft [3].Among all common methods for measuring the friction coefficient, the ring compression test has gained wide acceptance. This technique utilizes the dimensional changes of a test specimen to arrive at the magnitude of friction coefficient. A flat ring specimen is plastically compressed between two flat plates, increasing friction results in an inward flow of the material, while decreasing friction results in an outward flow of the material as schematically shown in Fig. 1.

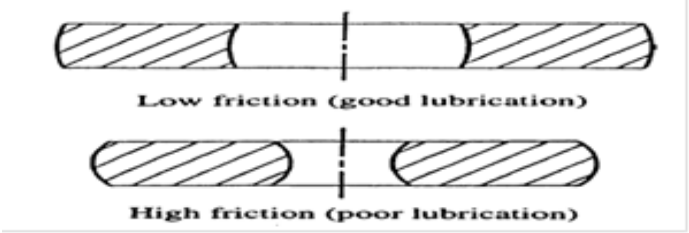

Fig. 1 Effect of friction magnitude on metal flow during the ring compression test

For a given percentage of height reduction during compression tests, the corresponding measurement of the internal diameter of the test specimen provides a quantitative knowledge of the magnitude of the prevailing friction coefficient at the die/ workpiece interface. If the specimen's internal diameter increases during the deformation, friction is low; if the specimen's internal diameter decreases during the deformation, the friction is high. Using this relationship, specific curves, later called friction calibration curves, were generated by Male and Cockcroft relating the percentage reduction in the internal diameter of the test specimen to its reduction in height for varying degrees of the coefficient of friction.as shown in Fig. 2.

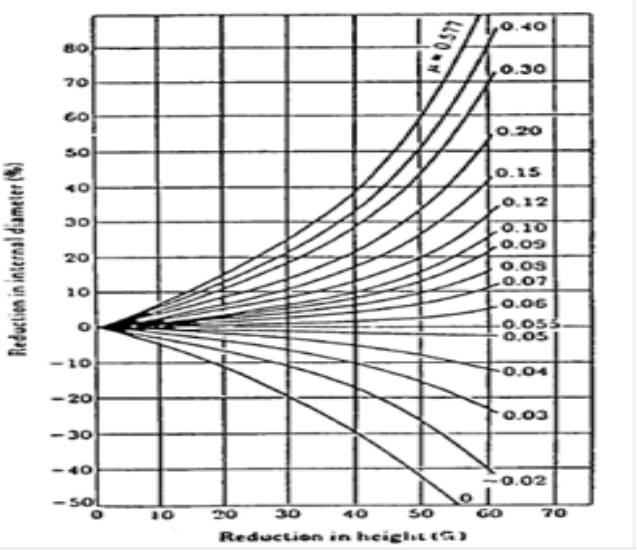

Fig. 2 Friction calibration curves in terms of μ Male and Cockcroft.

International Journal of Scientific & Engineering Research Volume 5, Issue 6, June-2014
ISSN 2229-5518

An attempt is made to address the dependency of the friction calibration curves obtained for the coefficient of friction and barreling. Steel [AISI 1010] material is used to conduct a number of ring compression tests. The non-linear finite element code ANSYS is used to simulate the ring compression test in order to investigate the effect of the above factors on the friction calibration curves.

2 Material and Method

Steel AISI 1010 is selected for the compression test analysis. The ring of outer diameter of 30mm, inner diameter of 15mm and height of 10mm as per the standard geometry(6: 3: 2) of Male and Cockcroft are used for the finite element analysis. The specimen is as shown in fig.3.

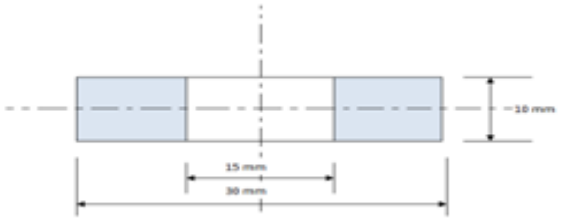

Fig.3. Ring specimen

Using the ANSYS code, one fourth of the specimen is modelled. The different height reductions and various coefficients of frictions in between die- work piece is provided. A number of simulations are carried out .and the profile obtained for inner nodes are investigated.

3 Numerical Analysis

The numerical analysis is carried out and finite element analysis (ANSYS). In an attempt to determine the frictional calibration curves of steel AISI 1010 under various conditions, ANSYS finite element code was employed in the simulation of simple compression of a cylindrical ring, 30 mm in outside diameter, 15 mm in inside diameter, and 10 mm in height. Due to the Axi-symmetric nature of this problem, as well as the existence of two axes of symmetry within each plane, a 2-D model representing one quarter of the cylindrical ring was constructed. A total of 631 2D 8-Node Structural Solid elements of type PLANE82 were used to model the billet specimen. The Holoman's stress- strain relation is used for ANSYS software coding .it's given as

$$\sigma = 103.8\ \epsilon^{0.22}\ ksi\ (Klb/in^2)$$
$$\sigma = 715.9086\ \epsilon^{0.22}\ N/mm^2$$

The contact between the specimen and the rigid compression platens was modelled via the *CONTACT PAIR option. The billet surface is modelled by CONTA172 option, while the rigid top and bottom compression platens were modelled using the TARJET 169 option. It is important to note that as the upper and lower compression platens approach each other, material originally on the lateral surface of the specimen moving in a radial direction may ultimately appear at the specimen-platen interfaces. It is thus necessary to lubricate the lateral surface of the specimen as well as the end surfaces and the platens in the experiments and to define interface element on the lateral surface of the billet in the finite element modelling. A rigid body reference node was defined at the rigid surface along the axis of the specimen to control the deformation rate. Fig.4. depicts the finite element model used in this analysis. Non linear approach is carried out.

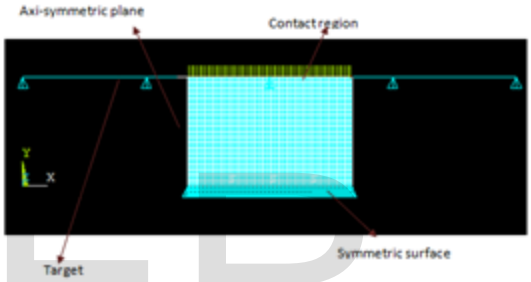

Fig. 4. Finite element model of ring compression test Specimen

In order to generate the friction calibration curves, deformation is made on target body in step by step as 0.5 mm, while the coefficient of friction was set at 0.02, 0.04, 0.06, 0.08, 0.1, 0.2, 0.3 and 0.4The friction calibration curves were then generated by plotting the percentage reduction in the internal diameter against the percentage reduction in the height of the model at different values of friction coefficient

4 Experemental Analysis

Cockcroft and Male Ring Compression test is used conduct the course of friction trials throughout this work, this method depends on the variations in the annular specimen's dimensions when subjected to compression. The reduction in height, increase or decrease of the internal diameter, external diameter determines the coefficient of friction under various lubrication conditions.

4.1 Specimen Material and Dimensions

Steel AISI 1010 is selected as the material. steel rod is machined under lathe. The specimens were cut to size as per the specification that is outer diameter: inner diameter: height as 6:3:2.and is all examined in the as-received conditions. To ensure similar surface roughness, the same cutting and prepara-

- *Asst.Prof. Libin Kochumman, SCTCE Trivandrum M.Tech in machine design.Kerala University, India, PH-+91 7403116172. E-mail: libinkochumman@gmail.com*
- *Prof. M R Sarathchandradas,Proffesor of P G studies in SCTCE Trivandrum, Kerala University, Kerala, India, PH-+91 9847945270 E-mail: sarat_chandradas@rediffmail.com*

International Journal of Scientific & Engineering Research Volume 5, Issue 6, June-2014
ISSN 2229-5518

tion techniques were applied to produce all the specimens.

Figure.5. steel specimen

Outer diameter of the specimen, D = 30mm
Inner diameter of the specimen, d = 15mm
Height of the specimen, H = 10mm

6.1 EXPERIMENTAL PROCEDURE

The Experimental procedure is followed over the range of all experiments. The Non-related parameters such as the compression speed, the die surface roughness, and the environment temperature and humidity, were all kept at constant values.

Procedure for dry condition

All examined specimens have the same dimension ratio of (OD: ID: H = 6 : 3 : 2). Initial thickness, specimen inner and outer radius (or diameters) were measured and recorded. Specimen freely placed on the lower die in a way that center lines of both coincided. The press then started pressing the specimen at a constant speed of (0.5 mm/min). When the specimen was compressed, it was released. The new thickness, inner and outer diameters were measured. However, due to barrelling and irregularity on both inner and outer cylindrical surfaces of specimen, several diametric readings are taken. It is continued for different load condition such as 600kN, 700kN, 800kN, 900kNand 1000kN.and readings are taken.

Procedure for lubricated conditions

In addition to the above steps, the specimen and dies contacting surfaces were lubricated before compression. The tests are carried out using lubricants, Zinc sterate, MoS_2 and Graphite powder.

5 RESULTS AND DISCUSSION

5.1 NUMERICAL RESULTS

The inner surface node deformation profile obtained for the steel ring specimen is shown in fig.6.to fig.8 which shows profile for 10%, 50%, and 90% height reduction.

The profile graph shown above, have similar node profile for each height reduction condition. The profile variation shows the inward and outward flow of metal respect to the friction coefficient. For these figures limits, of the coefficient of friction variation is obtained in between 0.02 to 0.4 its gives the transition of deformed node profile.

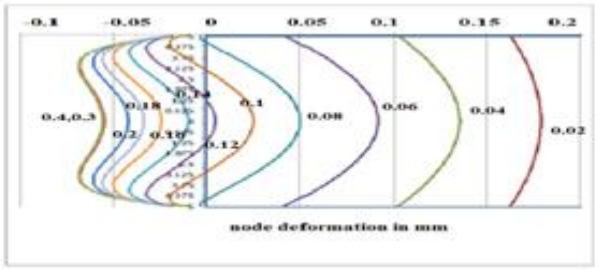

Fig.6 Node deformation profile for 10% height reduction for different coefficient of friction.

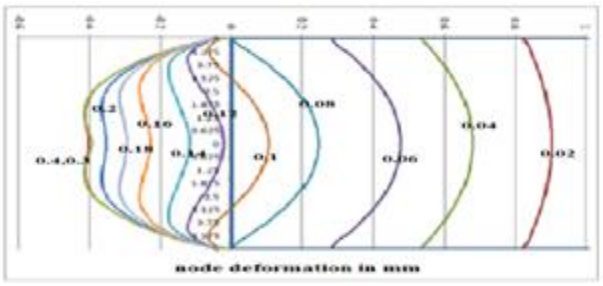

Fig.7 Node deformation profile for 50% height reduction for different coefficient of friction.

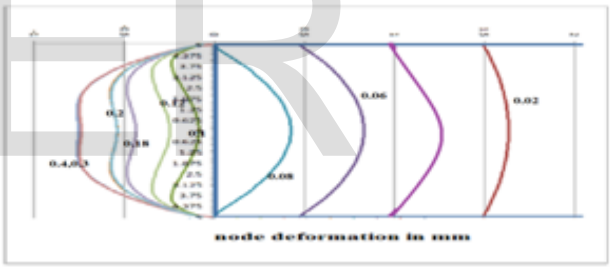

Fig.8 Node deformation profile for 90% height reduction for different coefficient of friction.

Please note that math equations might need to be reformatted from the original submission for page layout reasons. This includes the possibility that some in-line equations will be made display equations to create better flow in a paragraph. If display equations do not fit in the two-column format, they will also be reformatted. Authors are strongly encouraged to ensure that equations fit in the given column width.

5.2 STRESS VARIATION ANALYSIS

Inner node deformation is mainly created due to the stress acting on the inner diameter elements. Such analysing these stress variation give brief picture about the barrelling effect created under different lubrication. The contribution towards the barrelling under different lubrication is analysed based on this stress analysis. Stress acting in X direction in inner radius node for different lubrication at 10%, 50% and 90%height reduction for different coefficient of friction are shown in fig.9 fig.11.

International Journal of Scientific & Engineering Research Volume 5, Issue 6, June-2014
ISSN 2229-5518

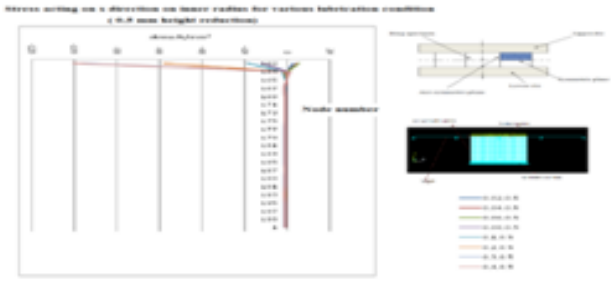

Fig.9 Stress acting on x direction in inner radius node for different lubrication at 10% height reduction

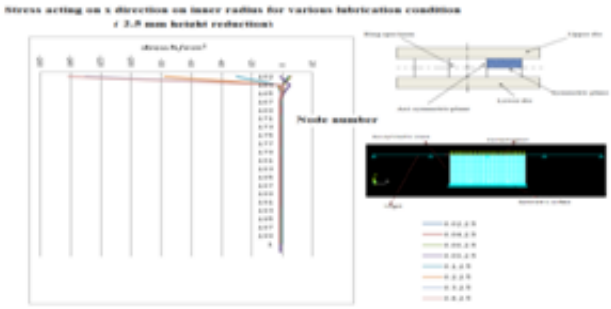

Fig.10 Stress acting on x direction in inner radius node for different lubrication at 50% height reduction

Fig.11 Stress acting on x direction in inner radius node for different lubrication at 90% height reduction.

The contact node has more variation compared to other nodes, after that stress variation remains a constant level as in fig.9 to fig.11.

Stress acting on y direction in inner radius node for different lubrication at various height reduction as shown in fig.5.20 tofig.5.22. From theses it can be analysed that, the inner node deformation is mainly created due to the stress acting on y direction. Since x directional stress controls the contact node deformation, y directional stress controls the deformation of other nodes. Fig.12 to fig.14 shows stress acting on y direction in inner radius node for different lubrication at 10%, 50% and 90% height reduction.

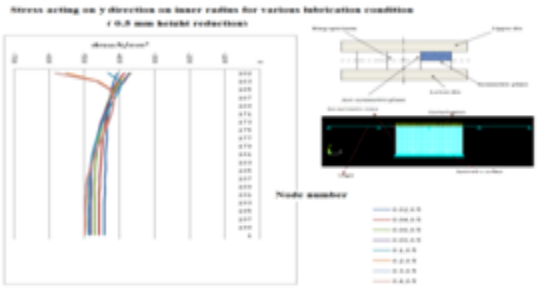

Fig.12 Stress acting on y direction in inner radius node for different lubrication at 10% height reduction.

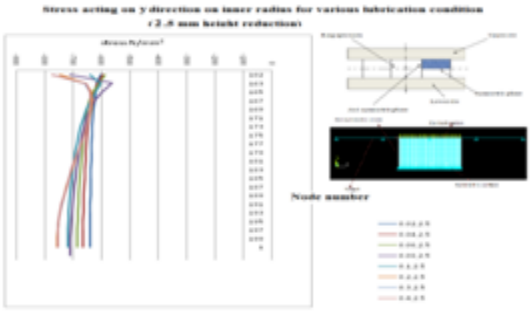

Fig.13 Stress acting on y direction in inner radius node for different lubrication at 50% height reduction.

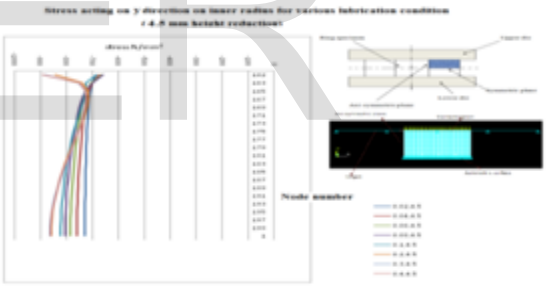

Fig.14 Stress acting on y direction on inner radius node for different lubrication at 90% height reduction.

Vonmisses stress variation is shown in fig.15 to fig.17 in which give combined stress variation.

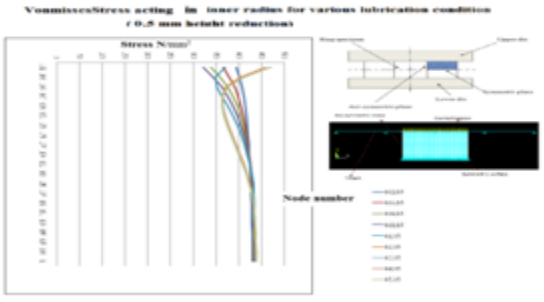

Fig.15 Vonmisses stress acting on inner radius node for different lubrication at 10% height reduction.

International Journal of Scientific & Engineering Research Volume 5, Issue 6, June-2014
ISSN 2229-5518

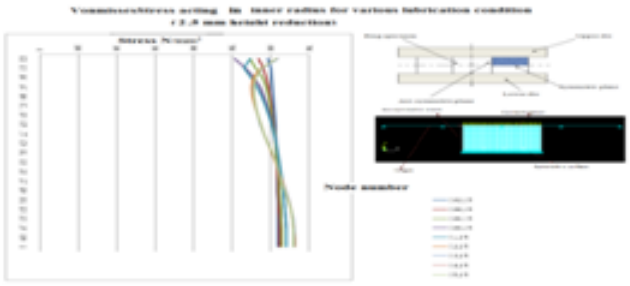

Fig.16 Vonmisses stress acting on inner radius node for different lubrication at 50% height reduction.

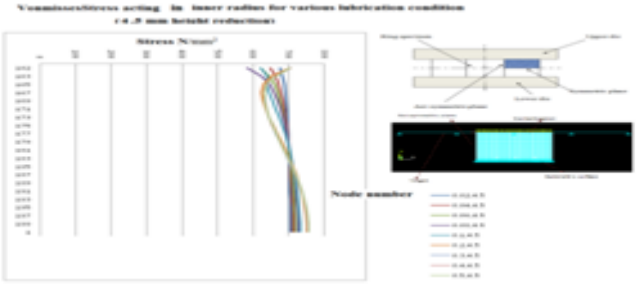

Fig.17 Vonmisses stress acting on inner radius node for different lubrication at 90% height reduction.

The friction curves obtained for steel ring for different friction condition for applied height reduction are obtained. Fig.6 to fig.17 graphs shows similar variation in deformation profile and stress variation, which indicates that the above friction coefficient 0.3 there is no significant variation in metal flow. That shows that friction coefficient above 0.3 shows similar inner diameter change. Below 0.3 the variation in inner diameter is present. The flow of metal is inward. As the friction coefficient reduces the metal flow become outward. The friction curve for the each friction condition is shown in fig.18, Thus friction curve obtained for Steel AISI 1010.

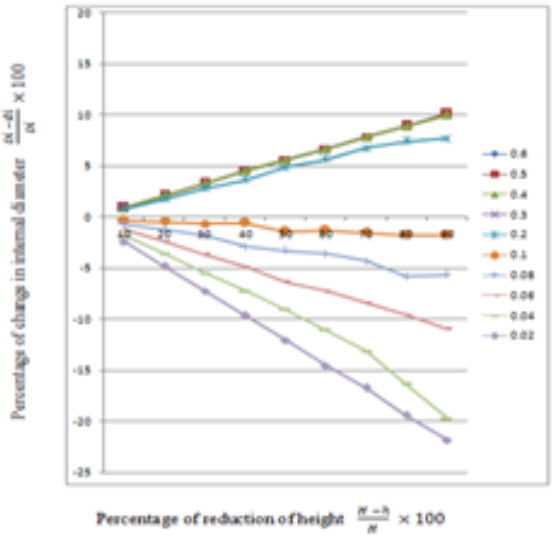

Fig.18. Friction calibration curve for Steel AISI 1010

6.3 EXPERIMENTAL RESULTS

The result obtained by experimental analysis is as shown in table 1

TABLE 1
RESULT OBTAINED BY EXPERIMENTAL ANALYSIS

	Load kN	% change in inn dia	% change in height
Dry condition	600	1.066	23.2
	700	1.466	32
	800	3.866	36
	900	4.266	45.6
	1000	5.533	51
Zinc sterate	600	-3.866	22.2
	700	-4.133	27.4
	800	-4.266	36
	900	-4.66	39
	1000	-5.066	43.2
MoS_2	600	-6.53	20.4
	700	-6.8	33.4
	800	-6.93	37
	900	-7.466	39.8
	1000	-8	45
Graphite powder	600	-0.66	23.8
	700	-2.133	26
	800	-2.66	36
	900	-4.533	37.2
	1000	-4.8	44

Fig.19 deformed specimen after loading for specified lubrication condition

The friction curve obtained for four lubrication condition is shown in fig.20

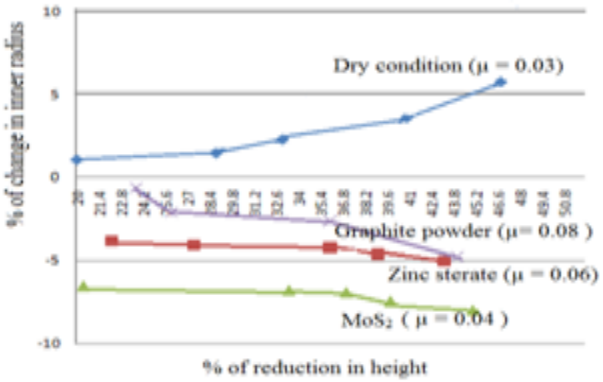

Fig.20 combined friction curves for steel AISI 1010

International Journal of Scientific & Engineering Research Volume 5, Issue 6, June-2014
ISSN 2229-5518

Comparison made between the numerical and experimental analysis is shown in fig21 to fig.24.

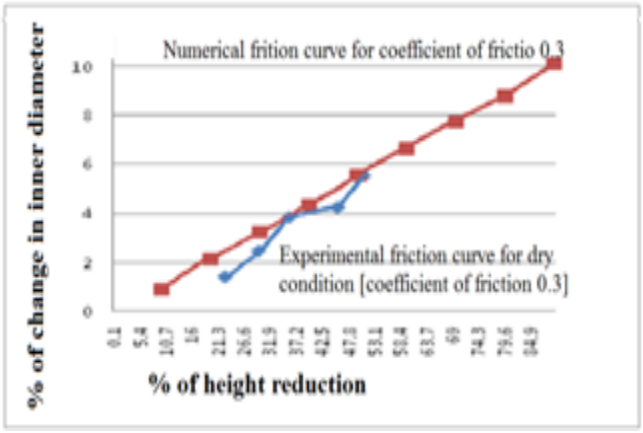

Fig.21 comparison of friction curve- numerical coefficient of friction 0.3 and dry condition

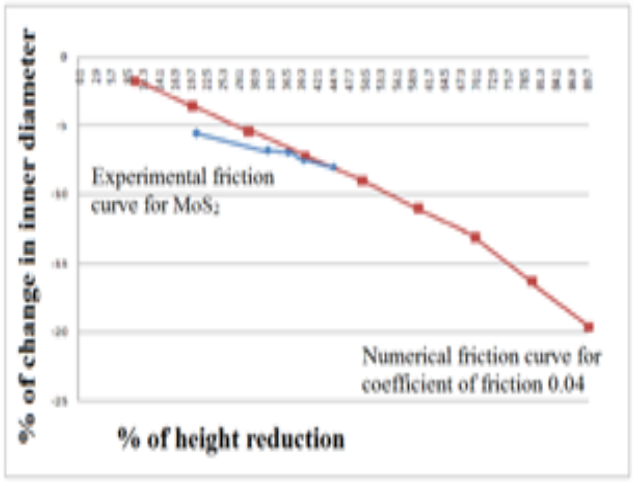

Fig.24 comparison of friction curve numerical coefficient of friction 0.04 and MoS_2 lubrication.

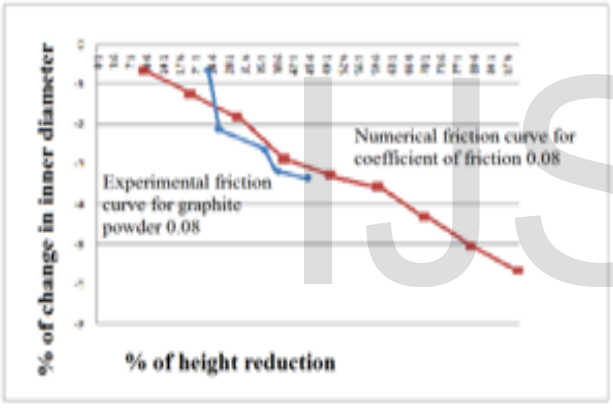

Fig.22 comparison of friction curve- numerical coefficient of friction 0.08 and graphite powder lubrication.

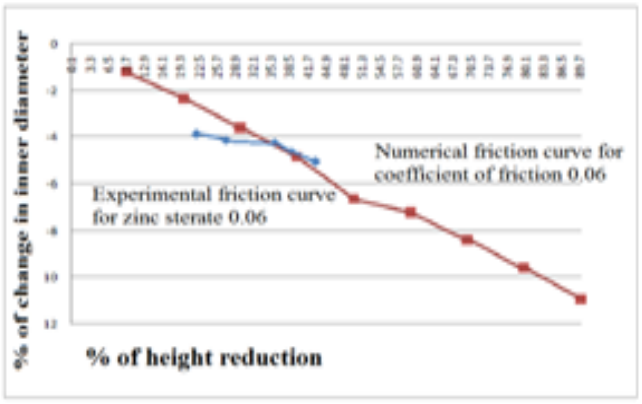

Fig.23 comparison of friction curves- numerical coefficient of friction 0.06 and Zinc sterate lubrication

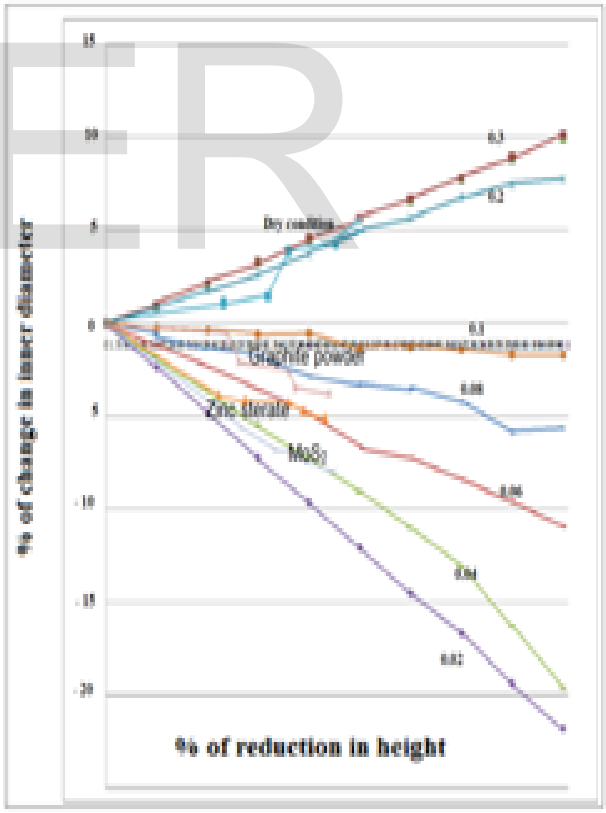

Fig.25 The result obtained by numerical and experimental analysis

The comparison is made for the result obtained by numerical and experimental analysis the fig.25 shows the result obtained by numerical and experimental analysis.

International Journal of Scientific & Engineering Research Volume 5, Issue 6, June-2014
ISSN 2229-5518

7 Conclusion

The frictional effect in the ring compression test is studied using FE simulation. Using the Finite element modelling Steel AISI 1010, ring compression test is carried out for different lubrication condition. For different coefficient of friction the friction calibration curves are obtained. Using lubricant zinc sterate, molybdenum di sulphide, graphite powder and dry condition the ring compression test is carried out experimentally and the friction curves are obtained. The coefficient of friction value obtained experimentally for dry condition is 0.3, for Zinc sterate is 0.06, for Molybdenum di sulphide is 0.04 and for Graphite powder lubrication condition is 0.08. The results obtained experimentally and numerically are compared and the friction curve is validated. The friction curve is more useful for analysing the material behaviour on forging process and selecting the lubricant for the process. This curve valid for AISI 1010 material only as changing material coefficients of friction value is varying according to the lubricant. Using this friction curves we can predict the lubricant for forging or extrusion process and the deformation profiles are analyzed to reduce unwanted machining. The deformation and stress variation study is carried out for the inner radius of the ring and barrelling effect is defined by the deformation profile and stress analysis. These analyses are useful to analyse the material flow and profile variations for different lubrication.

Acknowledgments

The authors would like to thank Associate Prof. Anoop Kumar S and Prof. Anil Kumar S H for their support in this work. They appreciate the useful discussion with Mr. Vishnu V A and other colleagues in FEM simulation.

REFERENCES

[1] Lee C.H., Altan T. Journal of Engineering for Industry-Transactions of the ASME, (1972), 775.
[2] Hasan Sofuoglu, Jahan Rasty. Tribology International, 32, (1999), 327.
[3] Sofuoglu H, Gedikli H. Tribology International, 35, (2002), 27.
[4] Vesna MANDIĆ, FRICTION STUDIES UTILIZING THE RING COMPRESSION TEST - PART I. 8th International Tribology Conference, 8. - 10. October 2003., Belgrade, Serbia.
[5] Robinson T, Ou H, and Armstrong, C. G . J. Mater. Process. Technol., (2004), 153.
[6] Hayhurst D.R, Chan M.W. International Journal of Mechanical Sciences, 47, (2005). P. Tiernan a,∗, M.T. Hillery a, B. Draganescu b, M. Gheorghe, Modelling of cold extrusion with experimental verification, Journal of Materials Processing Technology 168 (2005) 360–366.
[7] N. Vidhya Sagar, K S Anand, A C Mithun and K Srinivasan, Friction factor of CP aluminium and aluminium–zinc alloys. Bull. Mater. Sci., Vol. 29, No. 7, December 2006, pp. 685–688. © Indian Academy of Sciences.
[8] Mahmoud S. Zaamout and Jamil A. Makhadmi, Interface Friction Factor for Commercial Purity AluminumForged Under Dry and Lubricated, Umm Al-Qura Univ. J. Sci. Med. Eng. Vol.19,No.2, pp.191 - 202 (2007)
[9] Ajay Kumar Kaviti, Om Prakash and P. Vishwanath, Friction calibration map for determination of equal frictional conditions, Advances in Applied Science Research, 2011, 2 (5): 279-289.